BJES Basrah Journal for Engineering Sciences

Basrah Journal for Engineering Sciences, Vol. 22, No. 1, (2022), 9-19

Original Article

Journal homepage: www.bjes.edu.iq
ISSN (Online): 23118385, ISSN (Print): 18146120

OPEN ACCESS

Experimental and Numerical Study of Flow Through Horizontal Wellbore of the 180 Perforation Phasing

Mohammed A. Mustafa [1,*], Qais A. Rishack [2], Mohammed A. Abdulwahid [3]

[1] *Department of Mechanical Engineering, College of Engineering, University of Basrah, Basrah, Iraq*
[2] *Department of Materials Engineering, College of Engineering, University of Basrah, Basrah, Iraq*
[3] *Thermal Mechanical Engineering Department, Basrah Engineering Technical College, Southern Technical University, Basrah, Iraq*
E-mail addresses: pgs2338@uobasrah.edu.iq , qais.rashck@uobasrah.edu.iq , mohw2016@stu.edu.iq
Received: 20 August 2021; Revised: 3 October 2021; Accepted: 15 October 2021; Published: 24 April 2022

Abstract

This paper demonstrates experimental and numerical studies to investigate in perforation pipes with a phasing 180° and perforation densities 9 spm in a horizontal wellbore. The experimental study was conducted to investigate the phasing angle 180° in a horizontal wellbore. The wellbore has an inner diameter of 44 mm, as well as the length of the pipe is 2 m. For this purpose, a simulation model was created in the wellbore using the ANSYS FLUENT simulation software by using the standard *k-ϵ* model and applied to the (CFD) with changing the axial flow from (40 - 160) lit/min and constant inflow through perforations from range (20 - 80) lit/min. Concerning the findings of this study, it was noticed that the total pressure drop (friction, acceleration, mixing) goes high as the total flow rate ratio increases. As well as, an increase of the inflow concerning the main flow rate ratio leads to an increase in the total pressure drop and a decrease in the productivity index. Furthermore, the percentage error of the total pressure drop between the numerical and experimental results in test 4 is about 5.4 %. Also, the average velocity goes high with increasing the total flow rates and the velocity keeps increasing along the length of the pipe until it reaches its maximum value at the end of the pipe due to the effect of the perforations. It was concluded that there are the numerical and experimental results reflected a good agreement concerning the study of the flow-through perforations at 180° angle in terms of pressure drop and apparent friction factor, etc.

Keywords: Horizontal wellbore, Mixing effect, Pressure drop, Perforation, Productivity index

https://doi.org/10.33971/bjes.22.1.2

1. Introduction

In our present time, the concept of developing horizontal well signifies a revolutionary technology in the field of oil industry. Moreover, a number of analytical and experimental works, on this concept, were published. Such works addressed various aspects of horizontal wells which are used in production. These aspects include the concepts of productivity indices, transient flow models, and cresting behavior. The horizontal wells productivity will be identified by the pressure drop within the wellbore, particularly if it were to compare the pressure drop to reservoir drawdown. Consequently, the reservoir drawdown changes, so does the production. Despite the fact that these methods ultimately provide insights into horizontal well behavior, only a limited number deals with the pressure drop down the wellbore by predicting infinite conductivity. The infinite conductivity ultimately assumes that, along the well, there is no pressure drop (the pressure drop has to be neglected because it is very small). On the other hand, the uniform influx argues that the influx is constant throughout the well. In this context, Dikken [1] proposed the first analytical model for a horizontal wellbore in a state, single-phase, and turbulent flow. It is concluded that the total production rate as a function of the wellbore length. Besides, it is true that the wall friction pressure drop represents the whole pressure drop within the horizontal wellbore.

As the velocity of flow through the perforations goes high, the momentum affects not only the accelerating pressure drop but also the frictional pressure drop. In this connection, a number of authors have addressed this part of the pressure drop in recent years [2, 3, 4]. Aside from that, drilled perforations take the form of roughness elements [5].

The first study of fluid mixing between internal and main flow was raised flow provided by Su and Gudmundsson [6]. It mainly examined the effect of the friction, perforation, acceleration, low mixing pressure, and roughness in a perforated horizontal wellbore with fluid flow through the perforation where two fluids are mixed at junctions. Using the experimental parameters on a perforated pipe has an inner diameter of 22.2 mm and a length of 2 m. Moreover, it has a perforation diameter of 3 mm, a density of 12 SPF, and a 60° phasing. The results explained that the friction wall drop of pressure is about 80 %, the flow mixing pressure drop (including perforation roughness) is about 5 %, while it was observed that the pressure drop's acceleration records 15 % of the whole pressure drop. Another study in this regard was conducted by Schulkes and Utvik [7] who examined the total perforated horizontal pipes pressure drop, from 56 radial perforations, and figured out, by experimental calculation, the

effect of the inflow on the pressure drop as a result of acceleration process and mixing. The results obtained from the experimental data for a single-phase flow, the pipe diameter is 15 cm and the perforation diameter is 9 mm and 180° phasing. The findings of their study obviously reflected that the drop in the mixing pressure has a percentage of 10 % of the drop in the friction pressure. In a study conducted by Ouyang et al. [8] the significance of frictional and acceleration pressure drops in horizontal wells was investigated using a single-phase wellbore model. The results showed that the acceleration pressure differential may or, at times, may not be significant in comparison with frictional pressure. Subsequently, others [9,10,11] continued their research, and they proposed different coupling models of the well effect of pressure drop on the productivity ratio of a horizontal wellbore with single-phase flow. However, in some case studies, only the friction component is observed to identify the pressure drop across the wellbore. The most probable case; acceleration was considered when studying pressure drop, and other effects such as flow, mixing, etc. were ignored.

Wang et al. [12] presented a pressure gradients experimental model which was created mainly for the varied mass flow inside perforated pipes, the inflow through the perforated holes causes a variable mass movement inside the horizontal well. Moreover, the experiment results obviously reflected that as the injection ratio is leveled up, the pressure drop increases. Abdulwahid et al. [13] conducted a study; a numerical study, in which the ANSYS FLUENT was employed on pipe, mainly when that pipe physical model becomes incompletely perforated, and the regular pipe has no perforation. Moreover, the pipe length was 1300 mm, its ID = 22 mm, its perforation phasing was 60°. Besides, its perforation density was 6 SPF, while the Reynolds number moved from 28773 to 90153. The study conclusion strongly stated that the whole pressure drop increases through perforations, ultimately lead to a larger acceleration pressure drop concerning a higher flow rate. Moreover, the increase in perforations number absolutely increases the level of pressure drop and vice versa. In this connection, a study by Jing et al. [14] was conducted, in which the researchers analyzed the horizontal well variable mass flow. They presented both experimental and numerical perspectives. To do so, ANSYS FLUENT simulation software has been used. The results showed that the pressure drop goes high with increases in the flow rate of the perforating main pipe during the perforation process. A semi-analytical model was developed by Wanjing et al. [15] mainly to calculate a horizontal well's productivity index (PI) using pressure drop in addition to the wellbore. According to this study's results, a horizontal well's (PI) mainly relies on the interaction between Reynolds number, horizontal-well conductivity, and penetration ratio. The ratio of a high-permeability reservoir and an optimal penetration ratio might be found in the partial-penetration zone. Ping et al. [16] they have been suggested models for fluid flow in multi-branch horizontal wells with variable mass transfer. By incorporating the acceleration, friction, mixing, confluence, and gravity pressure drops, Newton-Raphson iterations, and Visual Basic programming. The result showed that in the proposed model, including the wellbore structure, the wellbore completion method, which significantly affected the wellbore pressure drop.

An empirical model was used in the research that differs from other models of previous researchers. Also, the effect of other factors in the horizontal wellbore, such as the productivity index and velocity distribution along the horizontal pipe, was calculated and compared with the numerical results.

The aim of this paper is to find out the main differences between the experimental results as well as the numerical results that highlight the effect of pressure drop along the perforated pipe. It also aims to calculate the effect of pressure drop (mixing, acceleration, and aggregate), friction factor, and productivity index through mathematical equations. It also attempted to calculate the effect of the through-perforation flow rate relative to the main flow on the productivity index of horizontal wells. This paper is organized as follows. The authors begin with some details of the theoretical background for an experimental device. Then followed the details of the numerical model and geometry along with a discussion of the relevant parameters affecting the theoretical background pressure loss.

2. Experimental work

Experiments were mainly conducted to determine the friction pressure drop, which is caused by wall friction and perforations roughness inside horizontal wells, because of the mixing of axial flow and radial flow (through perforation). Moreover, a special test section is made into a ring horizontal flow. The flow loop diagram is shown in Fig. 1 and the test pipe is obviously shown in Fig. 2.

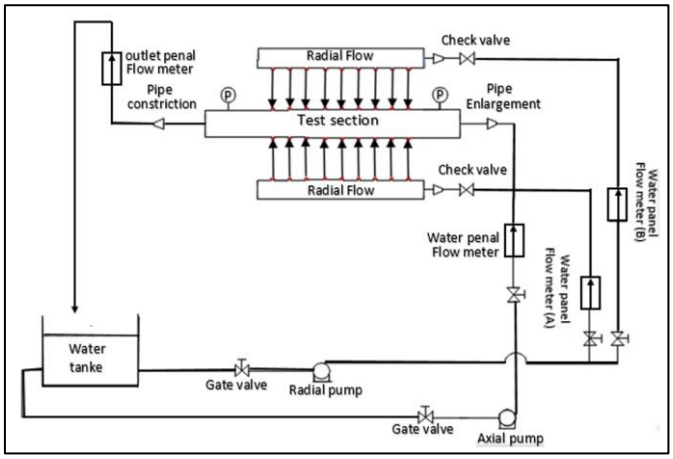

Fig. 1 the experiment apparatus schematic diagram.

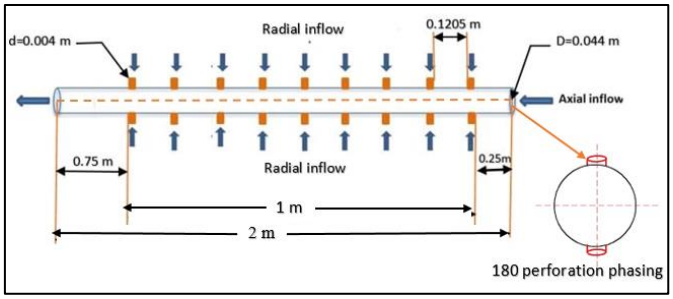

Fig. 2 the test pipe's schematic diagram.

This study experimental apparatus embodied two loops of water circulation; that is, the first loop works to supply water to the main pipe, while the other loop is used to the test pipe. Moreover, the test pipe is ultimately filled with water through the perforations.

The pipe is made from PVC. It has a 2 m length, 50 mm outer diameter along with 44 mm inner diameter. The test pipe

is perforated with 18 perforations and a perforations angle of 180°. The pipe is divided into three parts. The length of the perforated part is 1 m, and the length of the blank section is 0.25 m before the perforated section, and the length of the blank section is 0.75 m after the perforated section. The perforation diameter is 4 mm and the length of the perforation from the surface of the test pipe is 0.003 mm. Besides, the parameters of the main instruments are listed in Table 1.

Table 1. the main instrument's parameters.

Device	Tool specifications	Measurement range
Water panel flowmeter in the main pipe	PVC 1/2 in	40 – 160 lit/min
Water Panel flowmeter in inflow through perforations (A, B)	PVC 1/2 in	0.6 – 6 lit/min
Pressure sensor gauge	Stainless stales G1/4 NPT (male) 4-20 mA	0 –1.2 Mpa
Axial pump	CPm 158 2 HP	50 – 750 Lit/min
Radial pump	Dcd20 2 HP	30 – 500 Lit/min
Gate valve, check valve	PVC 1/2 in	-
Water storage tank	PVC	1/2 ton

The experimental apparatus is consisting of two pressure sensors, one before perforation and the other after perforation at a distance of 0.15 cm from each side of the pipe. Besides, the friction pressure drop in the test pipe was calculated by means of the pressure sensors. The pressure sensor has been connected to the Arduino and the Arduino has been linked to a screen in order to display the friction pressure for each point or in the image of the difference between two points.

3. Numerical simulations

The rapid advancement of computer technologies and software enables the solution of theoretical simulations for complex applications. This paper investigates a numerical analysis of a single-phase flow through a horizontal wellbore. The mathematical simulation with a 3D model with turbulent flow in the horizontal wellbore is performed using CFD ANSYS Fluent. The horizontal wellbore simulation is carried out using the conservation law (mass, momentum) in conjunction with the perturbation (k-ε) model. The finite volume method (FVM) solution of the continuity, momentum, and turbulence model equations is used to explain the calculation process of the control differential equation.

4. Description of the models

The numerical analysis is performed using ANSYS FLUENT and the standard k-ϵ model. Moreover, physical models are developed in the pipe of PVC, with perforation roughness of 0.03 mm. The test pipe has a perforated density of 9 spm with a perforations angle is 180°. The length of the pipe is drawing in ANSYS workbench has 2 m with 0.044 mm inner diameter and 4 mm perforation diameter as shown in Fig.3.

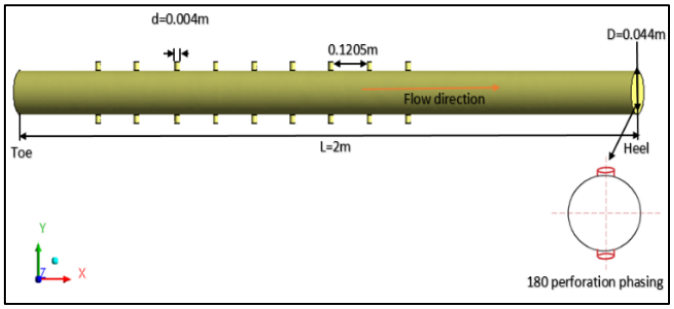

Fig.3 the physical model for 180° perforation phasing.

5. Simulation's parameters

The working fluid has 998.2 kg/m^3 constant density, 0.00103 kg/m.s dynamic viscosity and water at 25° of the water (isothermal). The results, which were conducted for a number of flow rates mainly to see the flow in perforated pipe, in all models, reflected the change in radial flow rate as 6 lit/min for each test. The details of the flow are summarized in Table 2.

The assumptions of the present are the phase is single, turbulent flow, steady state flow, Newtonian fluid, incompressible flow, and there is no transfer of heat between the system and its surrounding.

Table 2. the details of the flow.

Flow test	Axial flow (lit/min)	Radial flow (lit/min)
Test 1	40	20 – 80
Test 2	80	20 – 80
Test 3	120	20 – 80
Test 4	160	20 – 80

5.1. Governing equations

A perforated horizontal wellbore fluid flow undergoes a significant physical change, including pressure change as a result of friction losses in a horizontal pipe, acceleration, perforations, and mixing. To properly comment on such physical changes, (mass and momentum equations) are used as the fluid flow's two governing equations [18].

5.1.1. Mass's Conservation

The equation for mass's conservation is described as follows:

$$\rho \frac{\partial}{\partial x_i}(u_i) = 0 \tag{1}$$

5.1.2. Conservation of Momentum

In general, the momentum conservation equation is represented in Cartesian coordinates as follows:

$$\rho \overline{u_j} \frac{\partial}{\partial x_j}(\overline{u_i}) = -\frac{\partial \overline{P}}{\partial x_i} + \frac{\partial}{\partial x_j}\left(\mu\left(\frac{\partial \overline{u_j}}{\partial x_i} + \frac{\partial \overline{u_i}}{\partial x_j}\right) - \rho \overline{u_i' u_j'}\right) \tag{2}$$

Typically referred to as Reynolds-averaged Navier-Stokes.

To calculate the Reynolds stresses, employ the well-known Boussinesq relationship:

$$\overline{\rho u_i' u_j'} = \frac{2}{3} k \delta_{ij} - \mu_t \left(\frac{\partial \overline{u_j}}{\partial x_i} + \frac{\partial \overline{u_i}}{\partial x_j} \right) \quad (3)$$

Where:

δ_{ij} : represents the kronecker delta

Where the Kronecker delta, $\delta_{ij} = 1$ if $i = j$ and $\delta_{ij} = 0$ if $i \neq j$

5.2. Models of Turbulence (Standard k-ε model)

The standard *k-ε* model is related to the general class of two-equation models. Such models deal with two distinct transport equations. Moreover, they are most commonly adopted in industrial applications since they enjoy reasonable accuracy, economy, and robustness. Furthermore, the model's first major assumption tells that the turbulent viscosity μ_t is isotropic. The second major assumption claims that production and dissipation terms, which are given in the *k* equation, are said to be approximately equal at the local level [19].

The following *k*'s transport equations are used in the regular *k*-model;

$$\rho u_j \frac{\partial k}{\partial x_j} = \frac{\partial k}{\partial x_j} \left(\left(\mu + \frac{\mu_t}{\sigma_k} \right) \frac{\partial k}{\partial x_j} \right) + 2 \mu_t S_{ij} . S_{ij} - \rho \epsilon \quad (4)$$

and ϵ ;

$$\rho u_j \frac{\partial \epsilon}{\partial x_j} = \frac{\partial \epsilon}{\partial x_j} \left(\left(\mu + \frac{\mu_t}{\sigma_\epsilon} \right) \frac{\partial \epsilon}{\partial x_j} \right) + \mathrm{C}_{1\epsilon} \frac{\epsilon}{k} \mu_t S_{ij} . S_{ij} - \mathrm{C}_{2\epsilon} \rho \frac{\epsilon^2}{k} \quad (5)$$

The strain rate's tensor can be expressed as per velocity.

$$S_{ji} = \frac{1}{2} \left(\frac{\partial u_j}{\partial x_i} + \frac{\partial u_i}{\partial x_j} \right) \quad (6)$$

Besides, the terms of the boundary of the equation *k-ϵ* are listed as shown in the Table 3.

Table 3. Boundary conditions for the (*k-ϵ*) model.

Inlet	$K = \frac{3}{2} I^2 U^2 \quad ; \quad \epsilon = \frac{K^{0.5}}{0.3 D_h}$ Where I : is the specified turbulence intensity. D_h : is the hydraulic diameter of the inlet. The input is based on the mean value of the intensity is 5 % and the viscosity ratio μ/μ_t equal to 10.
Outlet, symmetry axis	$\partial k/\partial n = 0$ and $\partial \varepsilon/\partial n = 0$
Free stream	*k-ε* must be given or $\partial k/\partial n = 0$ and $\partial \varepsilon/\partial n = 0$
Solid walls	The approach depends on Reynolds number. Therefore, the velocity of the fluid at the wall's boundary is set to zero (No-slip B.C)

The constants were determined by fitting data intensively to the standard model *k-ϵ* for a wide range of turbulent flows. These equations include some constants [19]:

C_μ	σ_k	σ_ϵ	$C_{1\epsilon}$	$C_{2\epsilon}$
0.09	1.00	1.30	1.44	1.92

6. Theoretical model

There are three forms of whole pressure drop inside a perforated horizontal wellbore. The following relationship theoretically describes these groups.

$$\Delta P_T = \Delta P_f + \Delta P_{mix} + \Delta P_{acc.} \quad (7)$$

6.1. Friction Pressure Drop

Pipe wall friction creates a pressure drop due to a fluid's resistance to movement at the pipe wall. According to most researchers [6, 7, 13, 17], friction pressure drop has an important role as it accounts for the majority of the overall pressure drop, coming from the sum of (wall friction pressure and perforations roughness). The Darcy-Weisbach equation can be used to measure the frictional pressure in a horizontal wellbore.

$$\Delta P_{wall} = f_0 \frac{L}{D} \frac{\rho u^2}{2} \quad (8)$$

$$\Delta P_f = \Delta P_{wall} + \Delta P_{per} \quad (9)$$

f_t : represents the total friction factor for the pipe (dimensionless).
D : represents the main pipe's diameter (m).
L : length of pipe.

The friction pressure drop is calculated from the sum of the equation (9). We can calculate the friction pressure drop numerically and directly from the ANSYS Fluent.

6.2. Apparent Friction Factor (ft)

Truly speaking, the friction factor on the wall specifies the force, which is exerted by the fluid appearing on the wall in a turbulent flow, and different formulae are used for calculating the friction factor on the wall for smooth as well as rough pipes. Moreover, we can calculate the friction factor using the following equation:

$$f_t = f_o + f_p \quad (10)$$

Haaland equation [20] is the most valid and generally known formula for unperforated piping. The friction factor is expressed in turbulent flow as shown in the following equation:

$$\frac{1}{\sqrt{f_0}} = -1.8 \log \left(\frac{6.91}{Re} + \left(\frac{\epsilon}{3.7D} \right)^{1.11} \right) \quad (11)$$

The Reynold number is used to describe the ratio of inertia to viscous force. The friction factor of unperforated wellbore is calculated using the equation below.

$$Re = \frac{\rho u D}{\mu} \quad (12)$$

In fact, Asheim et al. [2], tend to provide a mathematical model which is mainly intended to determine the effective friction factor owing to inflow through perforations, using the equation below.

$$f_p = 4D\frac{q}{Q} + 2\frac{D}{n}\left(\frac{q}{Q}\right)^2 \quad (13)$$

The radial flow through perforation is calculated using the following equation:

$$q = n\frac{\pi}{4}d^2\, U_2 \quad (14)$$

6.3. Pressure Drop's Acceleration

The pressure drop, as it is caused by acceleration (momentum change), ultimately relies on the inflow radial velocity that occurs through the perforation. Besides, we can theoretically calculate the acceleration pressure drop as:

$$\Delta P_{acc.} = \rho\,(u_{out}^2 - u_{in}^2) \quad (15)$$

Where u_{in} , u_{out} the average velocity of the fluid, at both the inlet as well as the outlet of the pipe, respectively.

6.4. Mixing of Pressure Drop

The pressure drop occurs as a result of the mixing which is caused by perforation inflow. Besides, it is ultimately caused by the interaction between of main flow and inflow. That is, when the flow, through the perforations, blends with the main flow, enough energy is consumed for accelerating the inflow to the main pipe average velocity. Moreover, when the ratio's flow rate becomes greater than 0.0025, we can calculate the mixing pressure drop, using equations developed by Su and Gudmundsson [21]:

$$\Delta P_{mix} = 760\left(\frac{q}{Q}\right) \quad (16)$$

$\frac{q}{Q}$: The total ratio's flow rate (q) becomes the rate's total perforation flow, and it is divided by the rate's total flow at the pipe outlet.

6.5. Pressure Drop Coefficient

The coefficient of pressure drop is calculated as the proportion of the perforated pipe total pressure drop, divided by the change in kinetic energy, and at the outlet main pipe.

$$k = \frac{\Delta p}{0.5\,\rho\, U_{out}{}^2} \quad (17)$$

6.6. Productivity index (PI)

It is defined as PI (m^3/s / pa), the mathematical expression is resulting from dividing the amount of flow out of the main pipe by the total pressure drop as following.

$$PI = \frac{Q_3}{\Delta P_T} \quad (18)$$

7. Grid independence test

In order to verify the results of the numerical solution using the ANSYS FLUENT program. The maximum mesh size is determined in order to obtain the correct values in the first phase of the numerical simulation. In this study, the mesh is constructed using a CFD (Tetrahedron) with different maximum mesh sizes. The maximum mesh changing is used to show the best mesh properties that can be used for a simulation for all cases in this simulation. Three boundary layers are used on the wall of the pipe. Fig. 4 shows the structured computational grids.

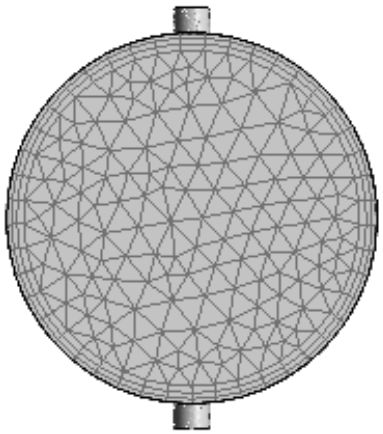

Fig. 4 Cross geometry of the test pipe.

The grid independence of all the mesh sizes is based on the average static pressure at two locations, the first location at a centerline along (x-axis) and the second location at the fluid domain as shown in Fig. 5.

The minimum percentage error of the predicted average static pressure lies between the previous and the next of the maximum mesh size of 0.00325 with 254372 nodes and 974705 elements. The percentage error between grid 12 and grid 13 for the two locations is 0.09 % for the centerline along (x-axis), 0.05 % for the fluid domain. The maximum mesh size of 0.00325 is used in the simulation in order to obtained good accuracy results. For checking quality, the determinant of an element obtained is equal to 0.79 at least.

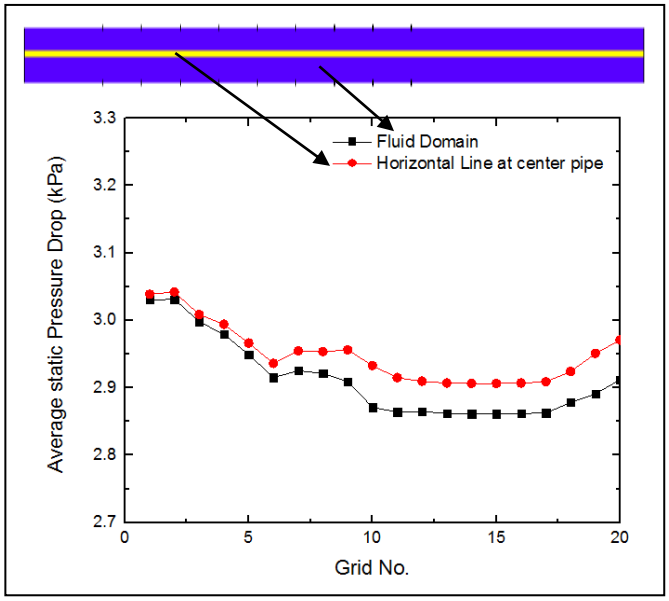

Fig. 5 Comparison of the average static pressure for varying mesh size.

8. Model validation

The research of Ruben m.s et al. [12] is used to validate the current study. CFD was used to simulate a perforated. Moreover, a 3-D horizontal pipe, which has 56 perforations, arranged in two lines of 28 perforations, and it is diagonally opposite each other, with a diameter of 0.009 m and a perforation phase angle of 180°. The pipe's length is 15 m, while the diameter is 0.15 m. This validation's boundary conditions are represented as follows: axial flow from 50 to 175 m^3/hr and the radial flow through perforation from change 0 - 2 m^3/hr.

Since fluid flow is the steady-state and incompressible flow, the ANSYS Fluent with the standard *k-ε* model is used. The validation results of the whole pressure drop along the pipe are very acceptable, as shown in Fig. 6. The figure clearly shows that 4.7 % is the maximum error, for the first flow test records zero flow rate ratio, and it decreases to 2.6 %, at total flow rate ratio which is equal to 0.183316. Moreover, flow test 2 reflects that 14.4 is the maximum error, at total flow rate ratio which is equal to zero, and it decrease to 5.5 % at total flow rate ratio equal to 0.624703.

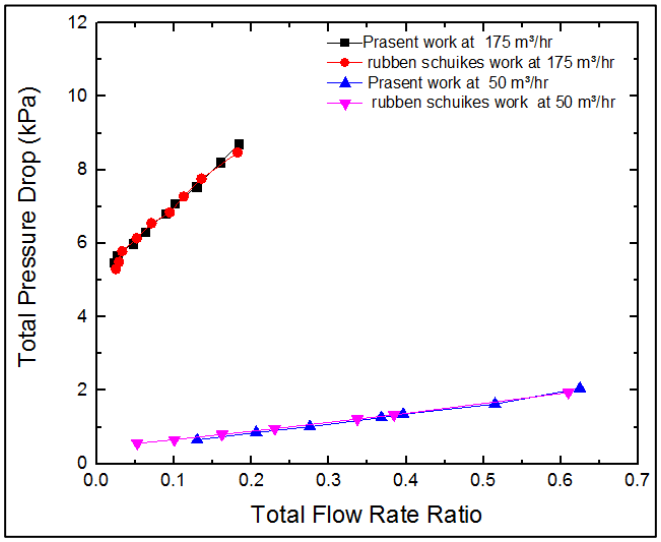

Fig. 6 Validation of present work with the Ref [12].

9. Results and Discussion

This paper takes the form of an experimental study. Besides, the experimental results are compared with the numerical results on the perforated pipe. The calculation is determined the effect of the perforation stages on the total pressure drop, acceleration, friction, and mixing. As well as, a study of apparent friction factors, productivity indexes, and velocity profiles. The study is conducted for several flow rates as illustrated in Table 2.

9.1. Pressure Drop in Perforation Pipe

Fig. 7 displays the connection between friction pressure drop and the overall ratio's flow rate. Moreover, the friction pressure drop appears resulting from the wall friction and perforation roughness. Thus, the friction pressure drop is representing by the experimental by taking the reading from the pressure sensor, comparing the experimental reading with the numerical data which computed from the CFD ANSYS FLUENT programs for several flow rates. It is observed that, in the true sense, the friction pressure drop increase as the flow rate ratio increases (an increase in radial flow for keeping the axial flow through the pipe constant). Besides, the frictional pressure drop goes high with an increase in Reynolds number. This is because of high velocity. This increase in friction pressure is caused by the effect of the shear stress on the wall. consequently, the increase in the flow rate as a result of flowing through the perforations. Moreover, the percentage error between experimental and numerical in the axial flow test is 40, 80, 120, 160 lit/min and radial flow from 20 - 80 lit/min is 6.88 %, 5.24 %, 5.85 %, and 3.32 %, respectively.

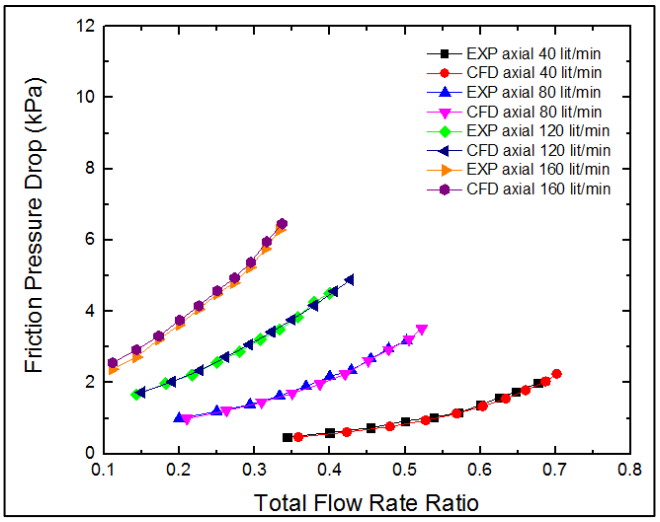

Fig. 7 Comparison between the experimental and numerical results of a friction pressure drop.

Fig. 8 represents the comparison between the experimental as well as the numerical results of the pressure drop's acceleration and the ratio's total flow rate. Thus, it is observed that the pressure drop's acceleration goes high with the overall flow rate ratio increases, because of the increase in outlet velocity caused by the increase in radial flow through the perforation. It is obviously observed that there is a slight difference in the acceleration pressure drop between the experimental and numerical values, because of the difference in velocity out of the horizontal wellbore.

Fig. 9 represents the comparison between the experimental and numerical results of the whole pressure drop as well as the ratio's total flow rate. It explains that the whole pressure drop goes high as the ratio's flow rate goes high. Moreover, it is seen that the increase in the total pressure is ultimately caused by an increase in the acceleration pressure drop because of an increase in flow rate ratio which is caused by radial flow through the perforation. Consequently, it is clearly observed that there is more wall friction because of the greater flow velocity taking place in the pipe. This happens by flowing inside the perforations and increasing the mixing effect, so the overall pressure increases. The percentage error between experimental and numerical in the several flow tests is 5.14 %, 5.65 %, 4.31 %, and 5.40 %, respectively.

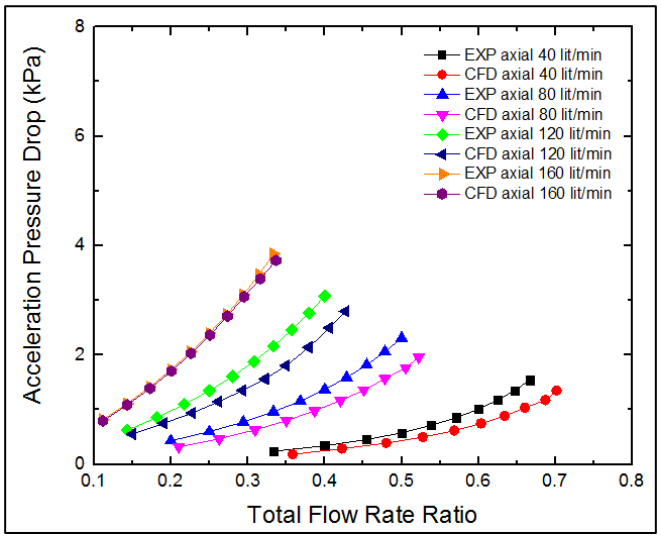

Fig. 8 Comparison between the experimental and numerical results of the acceleration pressure drop.

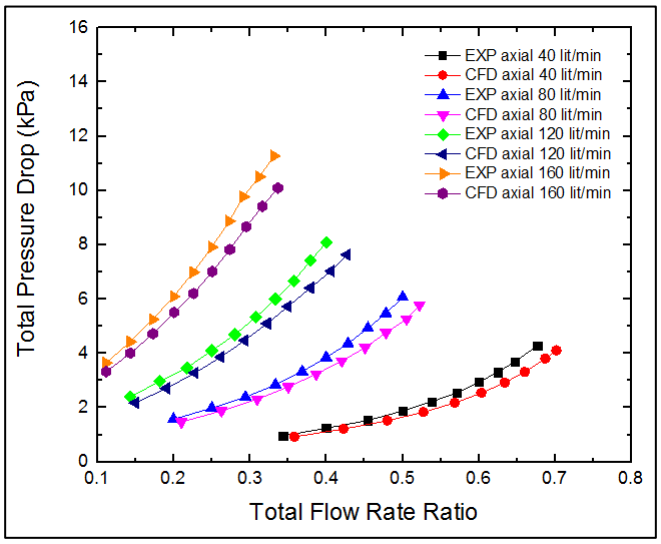

Fig. 9 Comparison between the experimental and numerical results of the total pressure drop.

Fig. 10 and 11 represent the parallel taking place between the experimental results on one side and the numerical results of the mixing pressure drop on the other side along with total ratio's flow rate. Besides, the mixing pressure drop was calculated from equation (16). The mixing pressure drop increases as the radial flow increases, which is due to an increase in outlet flow caused by the increase in flow during the perforation. It is noted that there is no obvious change between numerical and experimental results, due to the ratio of the flux between the perforations and the axial flow is little and the small diameter of the perforation. The mixing pressure drop for axial flow 40 lit/min and radial flow 20 - 80 lit/min is much higher than the mixing pressure drop for the other four flow tests. This is because the axial velocity in 40 lit/min is lower than the other tests, mixing pressure drop is higher for a lower axial flow.

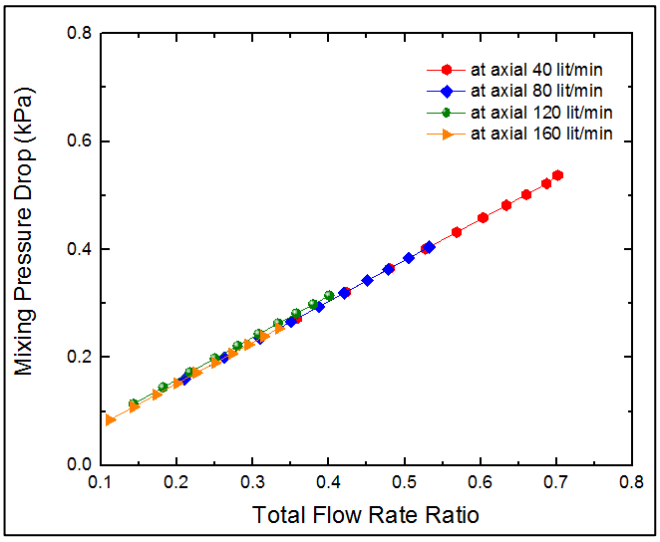

Fig. 10 Numerical mixing pressure drop with total flow rate ratio.

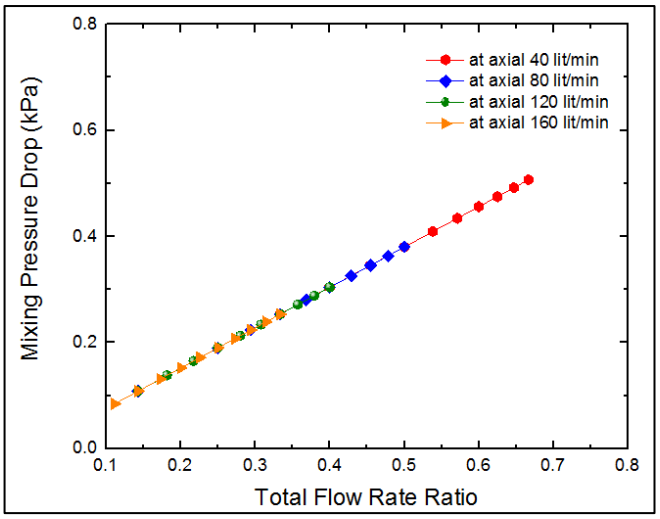

Fig. 11 Experimental mixing pressure drop with total flow rate ratio.

9.2. Static Pressure Drop

Fig. 12 represents the static pressure contour distribution along 2 m horizontal wellbore as the axial flow becomes 160 lit/min and the radial flow is 80 lit/min. Moreover, this figure shows that the pressure decreases gradually from the toe of the well to the heel of the well. Also, the pressure near the perforations represents the minimum value, because of higher density and viscosity in this area.

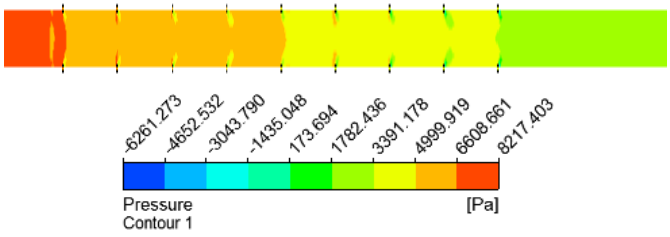

Fig. 12 the contours of pressure distribution along the pipe.

Fig. 13 represents the pressure drop along the centerline of the horizontal wellbore in several flow rates. It is noticed from the figure that as the value of axial flow increases when the radial flow through perforation remains constant at 80 lit/min. The static pressure increases at the inlet of the pipe as a result of the effect entrance, about 0.2 meters in the direction of the downstream and then a sudden decrease in pressure occurs at the site where the axial flow of the horizontal pipe meets the flow of the radial through the perforations until it reaches a constant value near the outlet pipe.

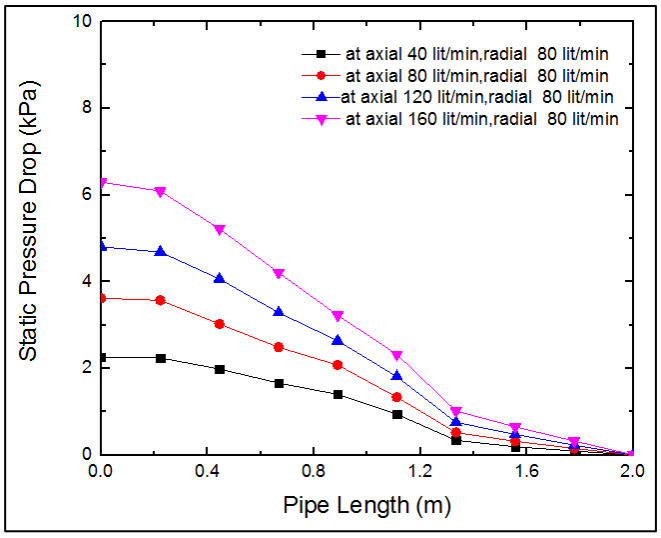

Fig. 13 Distribution static pressure drop along the pipe length.

9.3. Friction Factor

From the experimental results of the exit velocity and the measured friction pressure, the researcher calculated the noticed friction factor from the pressure drop, flow rate, through the test pipe as well as the pipe length, according to equation (10). The variation of the apparent friction factor, when comparison the experimental and numerical with a different radial flow rate is shown in Fig. 14. Besides, the apparent friction factor increases as the radial flow increases, because of the change in velocity field caused by inflow through perforations. Besides, the reduction in the velocity of flow near the wall, due to smaller wall pipe roughness. The axial and radial flow rates were selected from Table 2.

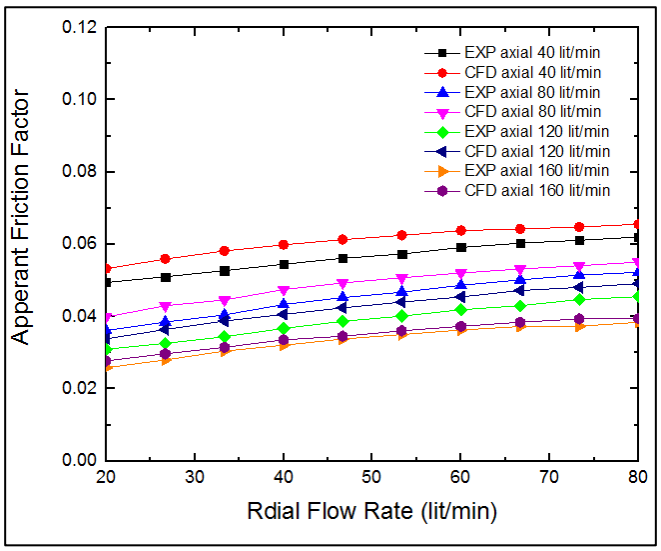

Fig. 14 Comparison between the experimental and numerical apparent friction factor with radial flow rate.

Fig. 15 represents the relationship that connects the friction factor, using the Haaland equation along with the total ratio's flow rate for different flow rates in the test pipe in Table 2. The Haaland friction factor decreases as the total ratio's flow rate increases, because of the increase in flow rate through the perforation and the effect of the roughness of the pipe reduces the effect of the friction factor.

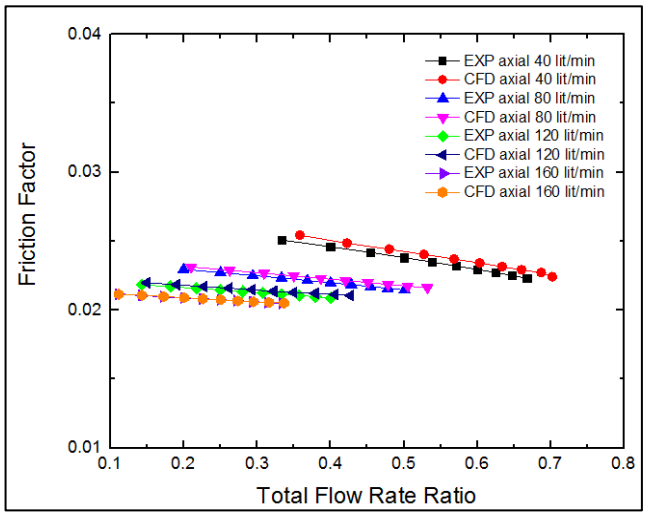

Fig. 15 Comparison the between experimental and numerical friction factor by Haaland equation.

9.4. Pressure Drop Coefficients

Fig. 16 illustrates the comparison results between the experimental and numerical for pressure drop coefficients and total ratio's flow rate. Moreover, the pressure drop coefficient was calculated by equation (17). The pressure drop coefficient increase linearly as the increases flow rate ratio. It is noticed that when the Re range goes high, the pressure drop increases, and the mass flow increases with high and low kinetic energy in the perforated pipe. The axial and radial flow rates were selected from Table 2. It is obvious that the coefficient of pressure drop, concerning test 1, is higher than other values of other tests. True enough, this is because of the axial velocity's lower values, at the entry of the pipe's perforation section. Hence, the coefficient of pressure drop goes high. Opposite to this, with the axial velocity's higher values, there exists a drop in the pressure drop coefficient's values.

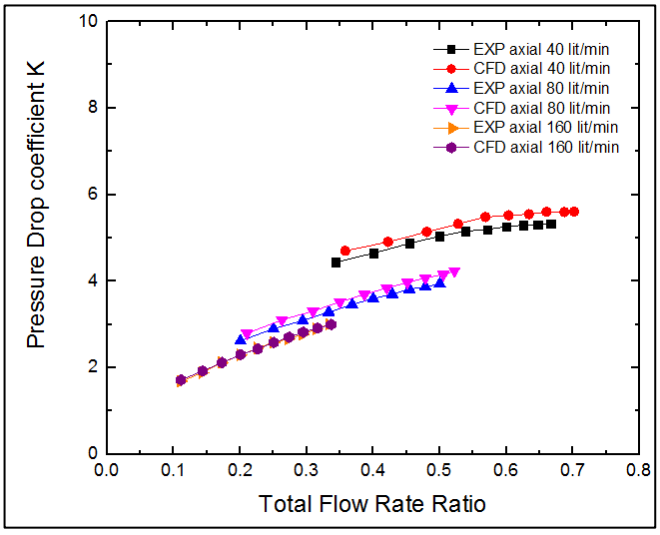

Fig. 16 Comparison between the experimental and numerical pressure drop coefficient.

9.5. Productivity Index

Fig. 17 represents the comparison between the experimental results as well as the numerical results of productivity index with total flow rate ratio for different flow rates. It is observed that the productivity index decreases with the leveling up of the ratio's total flow rate. The productivity index's decrease is caused by an increase in the total pressure drop along the pipe. Also, when the flow rate, during the perforations, goes high, the whole pressure drop increases more than the flow rate for the main pipe, this causes a decrease in the productivity index. The axial as well as radial flow rates were selected from Table 2.

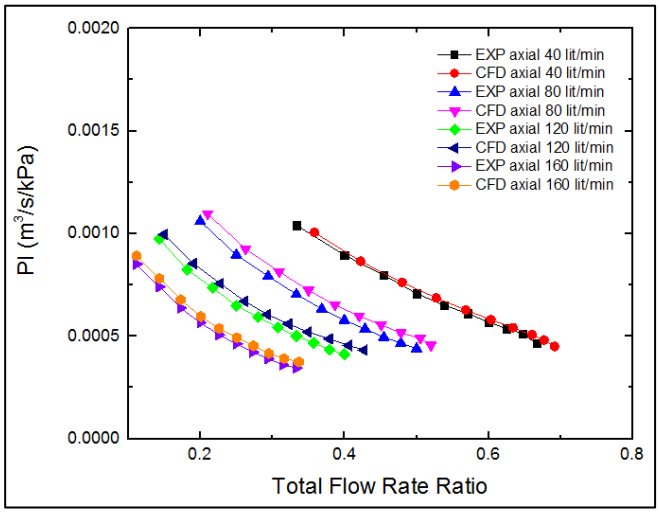

Fig. 17 Comparison between the experimental and numerical result of productivity index for different total flow rate ratio.

9.6. Average Velocity in the center-line of perforation pipe

Fig. 18 represents the relationship between the average velocity of the center-line of the pipe length in the test line for constant radial flow 80 lit/min and defines axial flow in Table 2. It is observed that the flow in the perforation disrupts the axial flow in the pipe, and this lead to increase in the velocity in the wellbore pierced from the toe tip to the heel tip due to the radial flow entering through the perforation as shown in Fig. 19. This figure explains the contour velocity distribution along the length pipe when the axial flow is 160 lit/min and the radial flow is 80 lit/min.

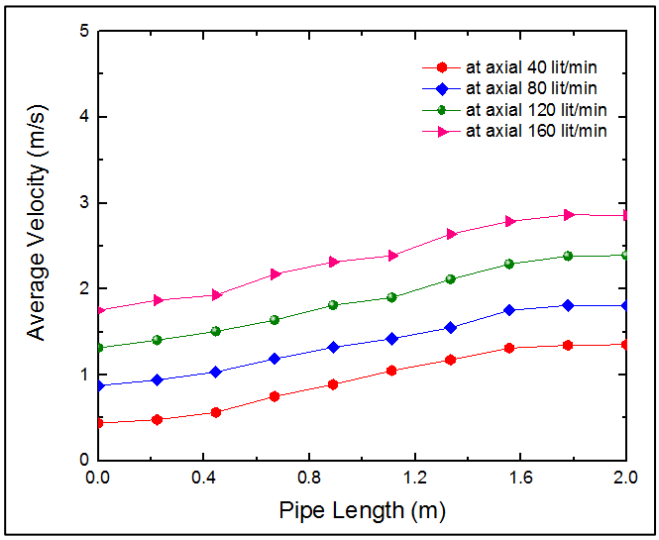

Fig. 18 the average velocity along the pipe length for different axial flow rate.

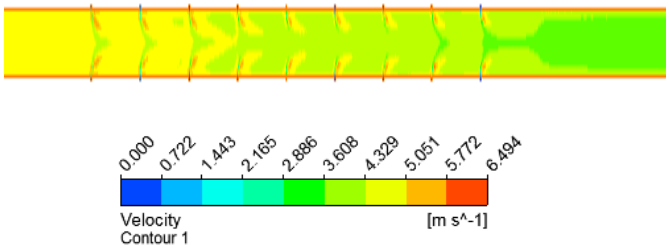

Fig. 19 the contours of velocity distribution along the pipe length.

9.7. Velocity Profile

Fig. 20 represents the velocity profiles in the direction of changing cross-sectional at various planes of the pipe when the axial flow rate of 160 lit/min and a radial flow rate of 80 lit/min. The figure shows the effect of radial flux on the axial velocity at different levels of the pipe. It is observed that the increase begins at the beginning of the wall and continues to increase until it reaches the center of the pipe and the velocity is the greatest in it, and after that, it begins to decrease until it reaches the end the pipe.

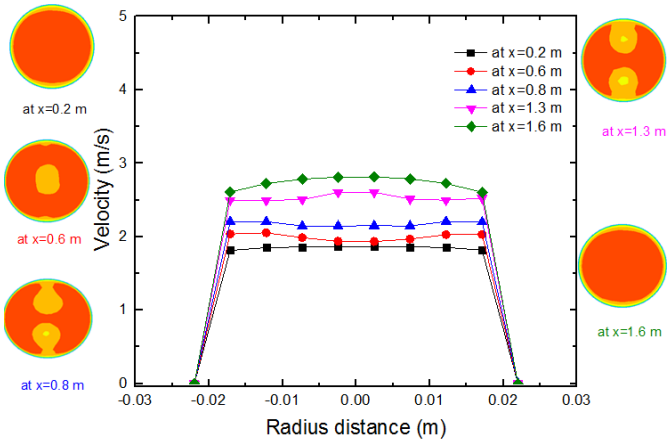

Fig. 20 the velocity profiles in the direction of changing cross section at various planes for the pipe.

10. Conclusions

An experimental and numerical study is conducted on perforation pipe with inflow during perforations in the horizontal wellbore. The experimental results were calculated from the device and obtained from the equations and compared with the numerical results for different flow rates in axial flow and inflow through the perforation. The numerical simulation of a perforation horizontal wellbore has been examined using ANSYS Fluent by using the standard ϵ model. It is noted that the numerical results are slightly higher than the experimental results. The study shows the following conclusions:

1. There is good agreement between the values measured from the experimental and numerical using ANSYS Fluent. So, the friction pressure drop increases with an increase in the ratio's total flow rate.
2. There is a little change in the acceleration and the total pressure drop for the experimental and numerical values. Thus, the increase in the total flow ratio brings about an increase in the total and acceleration pressure drop.

3. There is no difference in the mixing pressure drop between the experimental and numerical values calculated from the equations. It is noticed that the increase in the total flow ratio brings about an increase in mixing pressure.
4. There is, it is obviously shown in figures, an obvious change in apparent friction factor and pressure drop coefficient between experimental and numerical values.
5. There is a slight difference in the productivity index between the experimental and numerical values, because of the difference in velocity out of the pipe. So, the increase of the ratio of inflow to the main ratio's flow rate brings about a decrease in the productivity index.

Nomenclature

Symbol	Description	Unit
A	The pipe's cross-sectional area.	m^2
D	Main pipe diameter.	m
d	Perforation diameter.	m
ϵ	Roughness surface.	m
Q	Axial flow.	m^3/s
q	Radial flow through the perforation.	m^3/s
ΔP	Pressure drop.	kPa
μ	Fluid's viscosity.	kg/m.s
ρ	Fluid's density.	kg/m^3
f_t	Apparent friction factor.	-
PI	Productivity index.	-
n	Perforation density.	spm
u_i , v_i	Velocity vector.	-
μ_t	Eddy viscosity is also known as turbulent viscosity.	-
K	Represents the turbulent fluctuations of the kinetic energy.	-
S_{ij}	The mean rate of strain tensor.	-
ε	Turbulent dissipation rate.	m^2/s^3

References

[1] B. J. Dikken, "Pressure Drop in Horizontal Wells and Its Effect on Production Performance", J. Pet. Technol, Vol. 42, Issue 11, pp. 1426-1433, 1990. https://doi.org/10.2118/19824-PA

[2] H. Asheim, J. Kolnes and P. Oudeman, "A flow resistance correlation for completed wellbore", Journal of Petroleum Science and Engineering, Vol. 8, Issue 2, pp. 97-104, 1992. https://doi.org/10.1016/0920-4105(92)90048-6

[3] M. Ihara and N. Shimizu, "Effect of acceleration pressure drop in a horizontal wellbore", Society of Petroleum Engineers (SPE), the SPE Annual Technical Conference and Exhibition, Houston, 3-6 October 1993. https://doi.org/10.2118/26519-MS

[4] Z. Su, and J. S. Gudmundsson, "Friction Factor of Perforation Roughness in Pipes", the SPE Annual Technical Conference and Exhibition, Houston, Texas, October 1993. https://doi.org/10.2118/26521-MS

[5] H. Yuan, C. Sarica, and J. P. Brill, "Effect of Perforation Density on Single Phase Liquid Flow Behavior in Horizontal Wells", International conference on horizontal well technology, Society of Petroleum Engineers, SPE-37109-MS, November 18, 1996. https://doi.org/10.2118/37109-MS

[6] Z. Su, and J. S. Gudmundsson, "Pressure Drop in Perforated Pipes: Experiments and Analysis", the SPE Asia Pacific Oil and Gas Conference, Melbourne, Australia, SPE 28800, November 1994. https://doi.org/10.2118/28800-MS

[7] R. M. S. M. Schulkes, and H. O. Utvik, "Pressure Drop in a Perforated Pipe with Radial Inflow: Single-Phase Flow", SPE Journal, Vol. 3, Issue 1, pp. 77-85, 1998. https://doi.org/10.2118/38448-PA

[8] L. B. Ouyang, S. Arbabi, and K. Aziz, "A Single-Phase Wellbore-Flow Model for Horizontal, Vertical, and Slanted Wells", SPE Journal, Vol. 3, Issue 2, pp. 124-133, 1998. https://doi.org/10.2118/36608-PA

[9] E. Ozkan, C. Sarica and M. Haci, "Influence of Pressure Drop Along the Wellbore on Horizontal-Well Productivity", SPE Journal, Vol. 4, Issue 3, pp. 288-301, 1999. https://doi.org/10.2118/57687-PA

[10] W. Campos, R. C. Aguiar and D. Lopes, "Frictional and Accelerating Pressure Drops Effects on Horizontal Oil Well Productivity Index", 18th International Congress of Mechanical Engineering, November 6-11, 2005.

[11] F. Zeboudj and L. Bahi, "Horizontal Well Performance Flow Simulation CFD-Application", SPE Production and Operations Conference and Exhibition; Tunis, Tunisia, June 2010. https://doi.org/10.2118/133269-MS

[12] Z. M. Wang, J. N. Xiao, X. Q. Wang, and J. G. Wei, "Experimental study for pressure drop of variable mass flow in horizontal well", Journal of Experiments in Fluid Mechanics, Vol. 25, Issue 5, pp. 26-29, 2011.

[13] M. A. Abdulwahid, S. Dakhil and I. N. Niranjan Kumar, "Numerical Analysis of Fluid Flow Properties in a Partially Perforated Horizontal Wellbore", American Journal of Energy Engineering, Vol. 2, Issue 6, pp. 133-140, 2014. https://doi.org/10.11648/j.ajee.20140206.12

[14] J. Wen, M. Yang, W. Qi, J. Wang, Q. Yuan, and W. Luo, "Experimental analysis and numerical simulation of variable mass flow in horizontal wellbore", International Journal of Heat and Technology, Vol. 36, No. 1, pp. 309-318, 2018. https://doi.org/10.18280/ijht.360141

[15] W. Luo, Ch. Tang, and Y. Feng, "A Semianalytical Model for Horizontal-Well Productivity with Pressure Drop Along the Wellbore", SPE Journal, Vol. 23, Issue 5, pp. 1603-1614, 2018. https://doi.org/10.2118/189973-PA

[16] P. Yue, H. Yang, and Ch. He, G. M. Yu, J. J. Sheng, Z. L. Guo, C. Q. Guo, and X. F. Chen, "Theoretical Approach for the Calculation of the Pressure Drop in a Multibranch Horizontal Well with Variable Mass Transfer", ACS Omega, Vol. 5, Issue 45, pp. 29209-29221, 2020. https://doi.org/10.1021/acsomega.0c03971

[17] L. Hua, L. Yan, P. Xiaodong, L. Xindong, and W. Laichao, "Pressure Drop Calculation Models of Wellbore Fluid in Perforated Completion Horizontal Wells", International Journal of Heat and Technology, Vol. 34, No. 1, pp. 65-72, 2016. https://doi.org/10.18280/ijht.340110

[18] T. Vyzikas, "Application of numerical models and codes", A report prepared as part of the MERiFIC Project, Marine Energy in Far Peripheral and Island Communities, 2014.

[19] H. K. Versteeg and W. Malalasekera, An Introduction to Computational Fluid Dynamics, the Finite Volume Method, Second Edition, Pearson Education Limited, 2007. ISBN: 978-0-13-127498-3

[20] S. E. Haaland, "Simple and Explicit Formulas for the Friction Factor in Turbulent Pipe Flow", ASME, Journal of Fluids Engineering, Vol. 105, Issue 1, pp. 89-90, 1983. https://doi.org/10.1115/1.3240948

[21] Z. Su and J. S. Gudmundsson, "Perforation Inflow Reduces Frictional Pressure Loss in Horizontal Wellbores", Journal of Petroleum Science and Engineering, Vol. 19, Issue 3-4, pp. 223-232, 1998. https://doi.org/10.1016/S0920-4105(97)00047-8